AMERICAN SOCIETY FOR MICROBIOLOGY | mSphere®

RESEARCH ARTICLE
Host-Microbe Biology

Toxoplasma gondii AP2IX-4 Regulates Gene Expression during Bradyzoite Development

Sherri Huang,[a] Michael J. Holmes,[a] Joshua B. Radke,[c] Dong-Pyo Hong,[c] Ting-Kai Liu,[a] Michael W. White,[c] William J. Sullivan, Jr.[a,b]

Department of Pharmacology & Toxicology, Indiana University School of Medicine, Indianapolis, Indiana, USA[a]; Department of Microbiology & Immunology, Indiana University School of Medicine, Indianapolis, Indiana, USA[b]; Departments of Molecular Medicine and Global Health, University of South Florida, Tampa, Florida, USA[c]

ABSTRACT *Toxoplasma gondii* is a protozoan parasite of great importance to human and animal health. In the host, this obligate intracellular parasite persists as a tissue cyst that is imperceptible to the immune response and unaffected by current therapies. The tissue cysts facilitate transmission through predation and give rise to chronic cycles of toxoplasmosis in immunocompromised patients. Transcriptional changes accompany conversion of the rapidly replicating tachyzoites into the encysted bradyzoites, and yet the mechanisms underlying these alterations in gene expression are not well defined. Here we show that AP2IX-4 is a nuclear protein exclusively expressed in tachyzoites and bradyzoites undergoing division. Knockout of AP2IX-4 had no discernible effect on tachyzoite replication but resulted in a reduced frequency of tissue cyst formation following alkaline stress induction—a defect that is reversible by complementation. AP2IX-4 has a complex role in regulating bradyzoite gene expression, as the levels of many bradyzoite mRNAs dramatically increased beyond those seen under conditions of normal stress induction in AP2IX-4 knockout parasites exposed to alkaline media. The loss of AP2IX-4 also resulted in a modest virulence defect and reduced cyst burden in chronically infected mice, which was reversed by complementation. These findings illustrate that the transcriptional mechanisms responsible for tissue cyst development operate across the intermediate life cycle from the dividing tachyzoite to the dormant bradyzoite.

IMPORTANCE *Toxoplasma gondii* is a single-celled parasite that persists in its host as a transmissible tissue cyst. How the parasite converts from its replicative form to the bradyzoites housed in tissue cysts is not well understood, but the process clearly involves changes in gene expression. Here we report that parasites lacking a cell cycle-regulated transcription factor called AP2IX-4 display reduced frequencies of tissue cyst formation in culture and in a mouse model of infection. Parasites missing AP2IX-4 lose the ability to regulate bradyzoite genes during tissue cyst development. Expressed in developing bradyzoites still undergoing division, AP2IX-4 may serve as a useful marker in the study of transitional forms of the parasite.

KEYWORDS ApiAP2, apicomplexan parasites, differentiation, gene expression, intracellular parasites, transcription

Toxoplasma gondii is an obligate intracellular protozoan parasite that has infected up to one-third of the world's population (1). A key factor contributing to this parasite's widespread seroprevalence is its ability to transmit to new hosts through multiple routes (2). Felines are the definitive hosts that release infectious oocysts into the environment following infection. Oocysts, which are stable in the environment for up to 1 year, can be picked up by any warm-blooded vertebrate from contaminated soil or water (3). Upon ingestion, the sporozoites inside the oocysts are released, developing

Received 31 January 2017 **Accepted** 24 February 2017 **Published** 15 March 2017

Citation Huang S, Holmes MJ, Radke JB, Hong D-P, Liu T-K, White MW, Sullivan WJ, Jr. 2017. *Toxoplasma gondii* AP2IX-4 regulates gene expression during bradyzoite development. mSphere 2:e00054-17. https://doi.org/10.1128/mSphere.00054-17.

Editor Margaret Phillips, University of Texas Southwestern

Address correspondence to William J. Sullivan, Jr., wjsulliv@iu.edu.

Toxoplasma gondii AP2IX-4 regulates gene expression during bradyzoite development

into tachyzoites capable of infecting any nucleated cell (4). During an initial infection, *Toxoplasma* is also capable of crossing the placenta and potentially infecting the unborn fetus, resulting in spontaneous abortion or birth defects (5). Tachyzoites replicate asexually and can lead to the destruction of the host cell; alternatively, tachyzoites can differentiate into bradyzoites. Bradyzoite development is accompanied by slowed parasite growth and the formation of tissue cysts that can persist for long periods, perhaps for the lifetime of the host. New hosts can become infected when these tissue cysts are consumed through predation, which includes humans who eat raw or undercooked meat containing tissue cysts (2). Life-threatening episodes of acute toxoplasmosis most commonly arise in patients with compromised immune systems, such as in cases of HIV/AIDS, cancer chemotherapy, or organ transplantation, as a result of newly acquired or recrudescent infection (6). A better understanding of the molecular mechanisms that drive interconversion between tachyzoites and bradyzoites is required to manage transmission and pathogenesis of *Toxoplasma*.

Many studies have documented genes that are exclusively expressed in either tachyzoites or bradyzoites, suggesting that gene expression mechanisms play a major role in coordinating developmental transitions in *Toxoplasma*. Studies of stage-specific promoters revealed that conventional *cis*-acting mechanisms operate to regulate developmental gene expression during tissue cyst formation (7). The members of the principal class of transcription factors likely to work through these *cis*-acting promoter elements share features with the Apetala-2 (AP2) family in plants (8). In plants, the AP2 domain is composed of an ~60-amino-acid DNA-binding domain; plant factors with a single AP2 domain are linked to stress responses, whereas those with tandem AP2 domains are linked to plant development (9). However, more recent analyses of AP2 domains have been performed on additional species, including prokaryotes and free-living photosynthetic algae closely related to apicomplexan parasites. These data suggest that apicomplexan AP2 (ApiAP2) proteins originated in bacteria and expanded in myzozoans independently of those in plants, prior to the split between the *Apicomplexa* and chromerids (10).

Numerous ApiAP2 factors found in *Plasmodium* spp., *Toxoplasma*, *Cryptosporidium parvum*, and *Theileria annulata* are capable of binding specific DNA motifs (11–14), and several have been implicated as transcription factors involved in stage-specific gene regulation. In the rodent malaria parasite *Plasmodium berghei*, AP2-O activates gene expression in ookinetes (15), AP2-Sp regulates gene expression during the sporozoite stage (16), and AP2-L contributes to liver-stage development (17). PbAP2-G and PbAP2-G2 appear to work in conjunction to orchestrate transition of asexual blood-stage parasites to gametocytes (18). While PbAP2-G2 represses genes that are required for the proliferation of the asexual stage, PbAP2-G and its orthologue in *Plasmodium falciparum* function as master regulators that are essential for sexual stage development (19, 20). Those studies support the concept that transcriptional switches underlie developmental transitions between parasite life cycle stages. The work by Kafsack et al. also supports a stochastic model for gametocyte development, whereby spontaneous activation of PfAP2-G in some asexual stage parasites prompts transition to the sexual stage (20).

There are 67 predicted proteins in the *Toxoplasma* genome that harbor one or more AP2 domains (see ToxoDB.org), more than double the number found in *Plasmodium* spp. (21). In *Toxoplasma*, ApiAP2 factors have been found in association with chromatin remodeling machinery (22), and genetic studies have supported the idea of roles in regulating transcription in the context of developmental transitions from tachyzoites to bradyzoites (23–25). AP2IX-9, which is a stress-induced ApiAP2 factor, binds to *cis*-regulatory elements of bradyzoite promoters and operates as a repressor of bradyzoite development (23). In contrast, the AP2IV-3 stress-induced factor is an activator of bradyzoite gene expression and parasites lacking this factor display a reduced capacity to form tissue cysts *in vitro* (26). A knockout of AP2XI-4 impaired the activation of genes expressed during stress-induced differentiation and resulted in reduced cyst burdens in infected mice (24). Finally, AP2XII-6 was disrupted in a bradyzoite differentiation mutant

generated by insertional mutagenesis (25). To date, no master ApiAP2 factor has been identified in *Toxoplasma* that drives the unique transcriptome of any life cycle stage.

Here, we investigated the function of AP2IX-4, an ApiAP2 whose mRNA is upregulated during bradyzoite differentiation and exhibits cell cycle regulation. We show that AP2IX-4 protein is expressed in the parasite nucleus during the S/M phase. Surprisingly, genetic ablation of AP2IX-4 has no discernible effects on tachyzoites, and yet the knockout shows a reduced capacity to form tissue cysts *in vitro* and *in vivo*. These defects in developmental competency are reversed in a complemented knockout. AP2IX-4 is expressed in a subpopulation of bradyzoites that are undergoing division within a tissue cyst and acts to repress bradyzoite-associated genes. These findings underscore the complexity of the transcriptional program driving developmental transition to the bradyzoite stage and suggest that AP2IX-4 helps control the competing needs of parasite replication and tissue cyst formation.

RESULTS

AP2IX-4 is expressed in the nucleus during the S-M phase of the cell cycle. A previous study of predicted *Toxoplasma* ApiAP2 proteins revealed that AP2IX-4 (TGME49_288950) is 1 of 7 ApiAP2 genes whose mRNA is upregulated during alkaline stress (23) and exhibits cell cycle regulation in the tachyzoite (21). AP2IX-4 mRNA is one of the few ApiAP2 factors expressed at higher levels in day 21 tissue cysts purified from mice, and it is also robustly expressed during sporozoite meiosis (26). The single-exon AP2IX-4 gene is predicted to encode a 104-kDa protein consisting of 951 amino acids that harbors a single AP2 domain; no other protein domains were detected with SMART or InterPro protein sequence analyzers (27, 28).

We generated an endogenously epitope-tagged version of AP2IX-4 to confirm its size and expression pattern at the protein level and also to determine protein localization. RHΔ*ku80*::HXGPRT (RHQ) parasites were engineered to express native AP2IX-4 fused to a hemagglutinin (3xHA) tag at its C terminus (AP2IX-4^{HA}) (Fig. 1A). Western blotting of tachyzoite lysate showed that AP2IX-4^{HA} migrates as a single band at the expected size (Fig. 1B). Immunofluorescence assays (IFAs) were performed to detect subcellular localization and expression throughout the tachyzoite cell cycle while using the inner membrane complex-3 (IMC3) antibody to help delineate the cell cycle stages (29). AP2IX-4^{HA} protein was undetectable in the G_1 phase, appeared during the S-M stages, then decreased in expression during cytokinesis (Fig. 1C), consistent with its reported mRNA profile (21). Since the IMC3 staining pattern does not distinguish between the G_1 and S phases of the cell cycle, we quantified the proportion of vacuoles in G_1/S with no HA signal with respect to those in G_1/S with HA signal and in M/C with HA signal. The findings showed the proportions to be approximately 60%, 30%, and 10%, respectively, which is consistent with the distribution of G_1, S, and M/C cell cycle phases in an asynchronous tachyzoite population (Fig. 1D) (30). The IFA results also indicated that AP2IX-4^{HA} was exclusively present in the parasite nucleus when expressed (Fig. 1C).

AP2IX-4 is dispensable for tachyzoite replication *in vitro*. To investigate the function of AP2IX-4, we generated gene knockouts in RHQ and PruΔ*ku80*Δ*hxgprt* (PruQ) strains by replacing the genomic coding sequence (CDS) with a selectable marker dihydrofolate reductase-thymidylate synthase (DHFR*-TS) via double homologous recombination (Fig. 2A). Genomic PCRs were performed to screen transfected clones isolated by limiting dilution. Figure 2B shows the results, confirming successful allelic replacement of the *AP2IX-4* gene in the PruQ background (named the Δ*ap2IX-4* mutant). Reverse transcription-PCR (RT-PCR) was performed on mRNA harvested from Δ*ap2IX-4* parasites to verify loss of transcript (Fig. 2B). Parasite replication rates were determined using a doubling assay (Fig. 2C), and viability was examined using a plaque assay (Fig. 2D). Neither assay revealed a significant difference in the levels of *in vitro* growth between parental and Δ*ap2IX-4* parasites in the PruQ strain (Fig. 2C and D) or the RHQ strain (data not shown). These results suggest that, despite its appearance during the S-M stages of the cell cycle, AP2IX-4 is not required for tachyzoite replication.

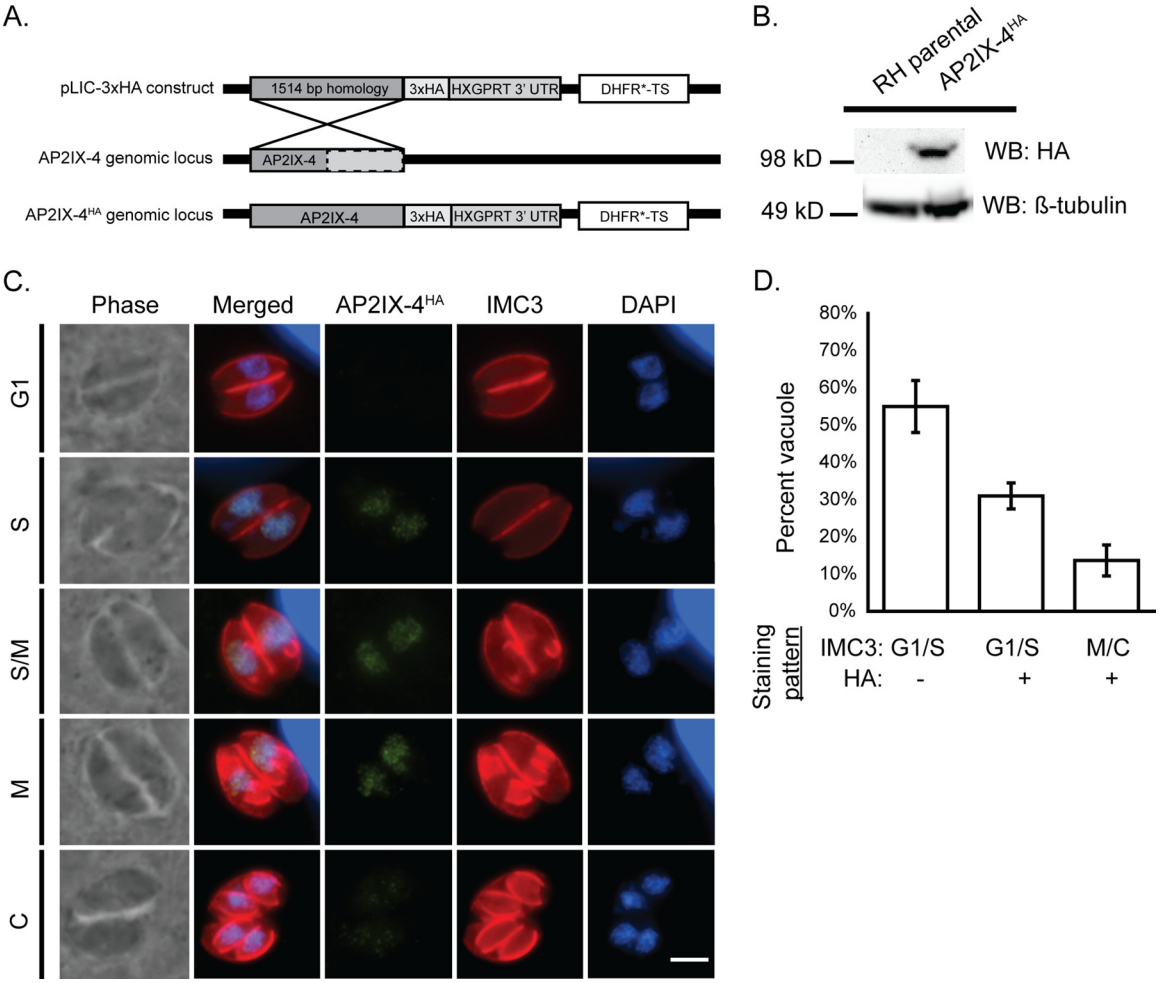

FIG 1 Characterization of AP2IX-4 protein expression. (A) Schematic showing the strategy used to generate parasites expressing AP2IX-4 tagged at the C terminus with 3xHA epitopes (AP2IX-4^{HA}) in RHQ parasites. The AP2IX-4 genomic locus is aligned with the pLIC-3xHA construct used for endogenous tagging via single homologous recombination. The construct contains a 1,514-bp homology region and a DHFR*-TS drug selection cassette. UTR, untranscribed region. (B) Western blot (WB) of parental RHQ and AP2IX-4^{HA} parasites probed with anti-HA antibody. Anti-β-tubulin was used to verify the presence of parasite protein. kD, kilodaltons. (C) IFAs performed on AP2IX-4^{HA} tachyzoites using anti-HA (green). To monitor cell cycle phases, parasites were costained with anti-IMC3 (red) and DAPI (blue). G1, gap phase; S, synthesis phase; M, mitotic phase; C, cytokinesis. Scale bar, 3 μm. (D) Quantification of the proportion of parasite vacuoles (of 100) in the asynchronous population of AP2IX-4^{HA} parasites exhibiting G_1/S IMC3 staining with absence of HA signal (G_1/S HA-), G_1/S IMC3 staining with positive HA signal (G_1/S HA+), or M/C staining with positive HA signal (M/C+). Error bars represent standard deviations of results from 3 independent experiments.

AP2IX-4 is present in bradyzoites and required for efficient cyst formation *in vitro*. Previous studies indicated that levels of AP2IX-4 mRNA increase during bradyzoite differentiation *in vitro* and that elevated levels of AP2IX-4 transcripts are present during the chronic stage of infection in mice (21, 31). To examine the function of AP2IX-4 in bradyzoites, we complemented the PruQΔ*ap2IX-4* parasites by targeting a cDNA-derived version of AP2IX-4 tagged with HA at its C terminus to be under the control of the native AP2IX-4 promoter (PruQΔ*ap2IX-4*::AP2IX-4^{HA}; Fig. 3A). Genomic PCRs confirmed integration of the complementation construct at the disrupted *ap2IX-4* locus (Fig. 3B), and Western blot analysis confirmed the expected size of the AP2IX-4^{HA} protein (Fig. 3C). Furthermore, the AP2IX-4^{HA} protein in the complemented knockout localized properly to the parasite nucleus during S-M phases (Fig. 3D), matching the pattern that we observed for native protein in RH parasites (Fig. 1C). The proportions of vacuoles in G_1/S with no HA signal relative to those in G_1/S with HA signal and in M/C with HA signal were approximately 60%, 30%, and 10%, respectively (Fig. 3E), consistent with observations made in the type I strain (Fig. 1D). Together, these data confirm the

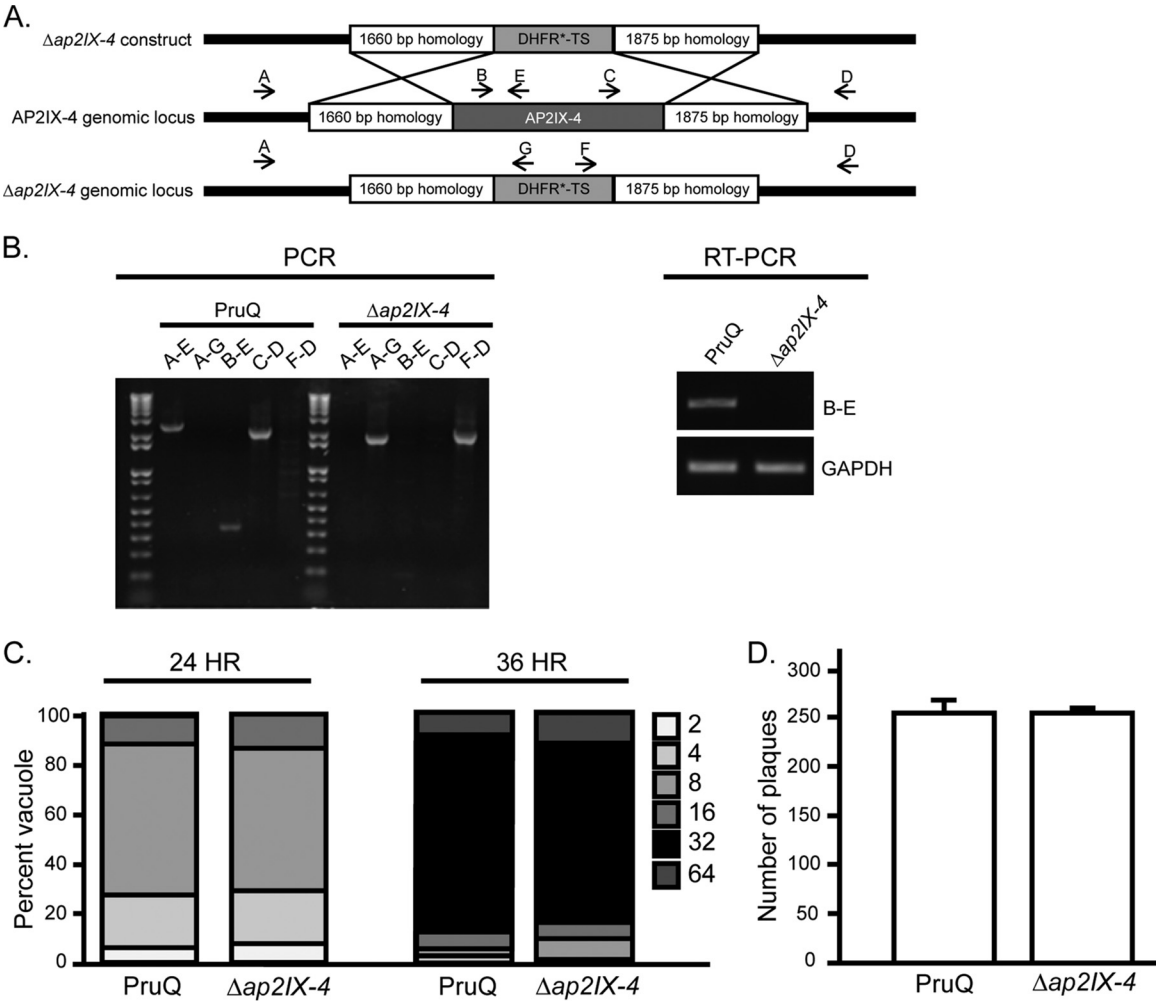

FIG 2 Generation of PruQΔ*ap2IX-4* parasites. (A) Schematic illustrating the generation of the AP2IX-4 knockout by allelic replacement with a DHFR*-TS minigene. (B) Genomic PCRs were performed with the indicated primers (A to G) to verify replacement of the AP2IX-4 genomic locus with the DHFR*-TS minigene. RT-PCR performed with primers B and E confirmed the absence of AP2IX-4 transcripts in PruQΔ*ap2IX-4* parasites. Primers for GAPDH were used as a positive control for the RNA preparation. (C) Representative doubling assay showing the number of parasites/vacuole at 24- and 36-h time points postinfection for parental PruQ versus PruQΔ*ap2IX-4* parasites. Three independent assays were performed with similar results. $P > 0.05$ (unpaired two-tailed Student's *t* test). (D) Plaque assays were performed to compare the *in vitro* viability of PruQ parasites to that of PruQΔ*ap2IX-4* parasites. Three independent assays were performed with similar results. $P = 0.98$ (unpaired two-tailed Student's *t* test).

fidelity of the complemented knockout and uncover no differences in localization or cell cycle regulation of AP2IX-4 between type I and type II strains.

Taking advantage of this HA-tagged version of AP2IX-4 in the developmentally competent type II strain, we monitored protein expression by IFA during alkaline stress (pH 8.2), a well-characterized inducer of tissue cyst development *in vitro* (32). The PruQ strain also contains a green fluorescent protein (GFP) reporter driven by the bradyzoite-specific LDH2 promoter (33, 34). Under alkaline stress bradyzoite induction conditions, expression of AP2IX-4^{HA} was heterogeneous within the population of bradyzoites housed in individual cysts (Fig. 4A). Comparing the number of AP2IX-4^{HA}-positive parasites to the total number of parasites within developing tissue cysts (among 50 random cysts in 3 independent replicates), we found that only 13% were expressing AP2IX-4^{HA} at 2 and 4 days postinduction. In contrast, 37% of tachyzoites expressed AP2IX-4^{HA}. Costaining for IMC3 revealed that GFP-positive bradyzoites expressing AP2IX-4^{HA} were in the process of dividing, revealing that AP2IX-4^{HA} expression continued to be regulated by the cell cycle during encystation (Fig. 4B). Loss of AP2IX-4 does not appear to have had a significant impact on the number of

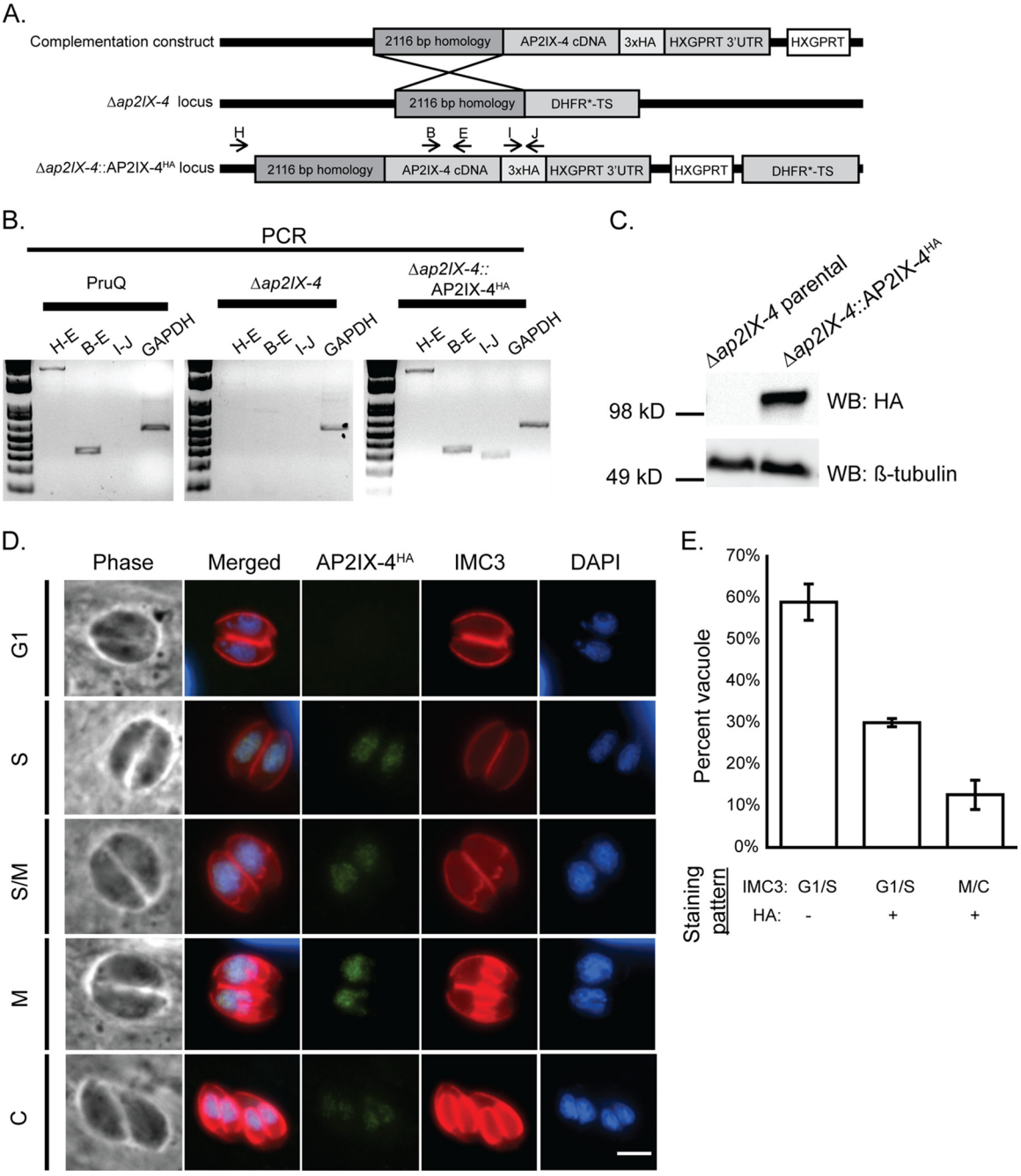

FIG 3 Complementation of the AP2IX-4 knockout. (A) Schematic illustrating the generation of the complemented knockout (Δ*ap2IX-4*::AP2IX-4^{HA}). A cDNA-derived version of AP2IX-4 tagged at the C terminus with 3xHA (complementation construct) was targeted to the ablated genomic locus in Δ*ap2IX-4* parasites. (B) Genomic PCRs were performed with the indicated primer pairs to confirm proper integration of the complementation construct into Δ*ap2IX-4* parasites. Primers corresponding to GAPDH were used as a positive control of the DNA preparation. (C) Western blot of Δ*ap2IX-4* and Δ*ap2IX-4*::AP2IX-4^{HA} parasites with anti-HA, using anti-β-tubulin as a control to verify the presence of parasite protein. (D) IFAs were performed on Δ*ap2IX-4*::AP2IX-4^{HA} tachyzoites as described for Fig. 1C. (E) Quantification of the proportion of parasite vacuoles (of 100) in the asynchronous population of AP2IX-4^{HA} parasites performed as described for Fig. 1D.

parasites undergoing division at day 4 of bradyzoite induction; the proportions of dividing parasites as assessed by IMC3 staining of 50 random cysts were 7.6% for PruQ parasites and 6.5% for PruQΔ*ap2IX-4* parasites.

We next examined the frequency of bradyzoite cyst development in parental PruQ and PruQΔ*ap2IX-4* parasites in response to alkaline stress, as determined by the number of vacuoles staining positive for cyst wall protein binding *Dolichos* lectin. After

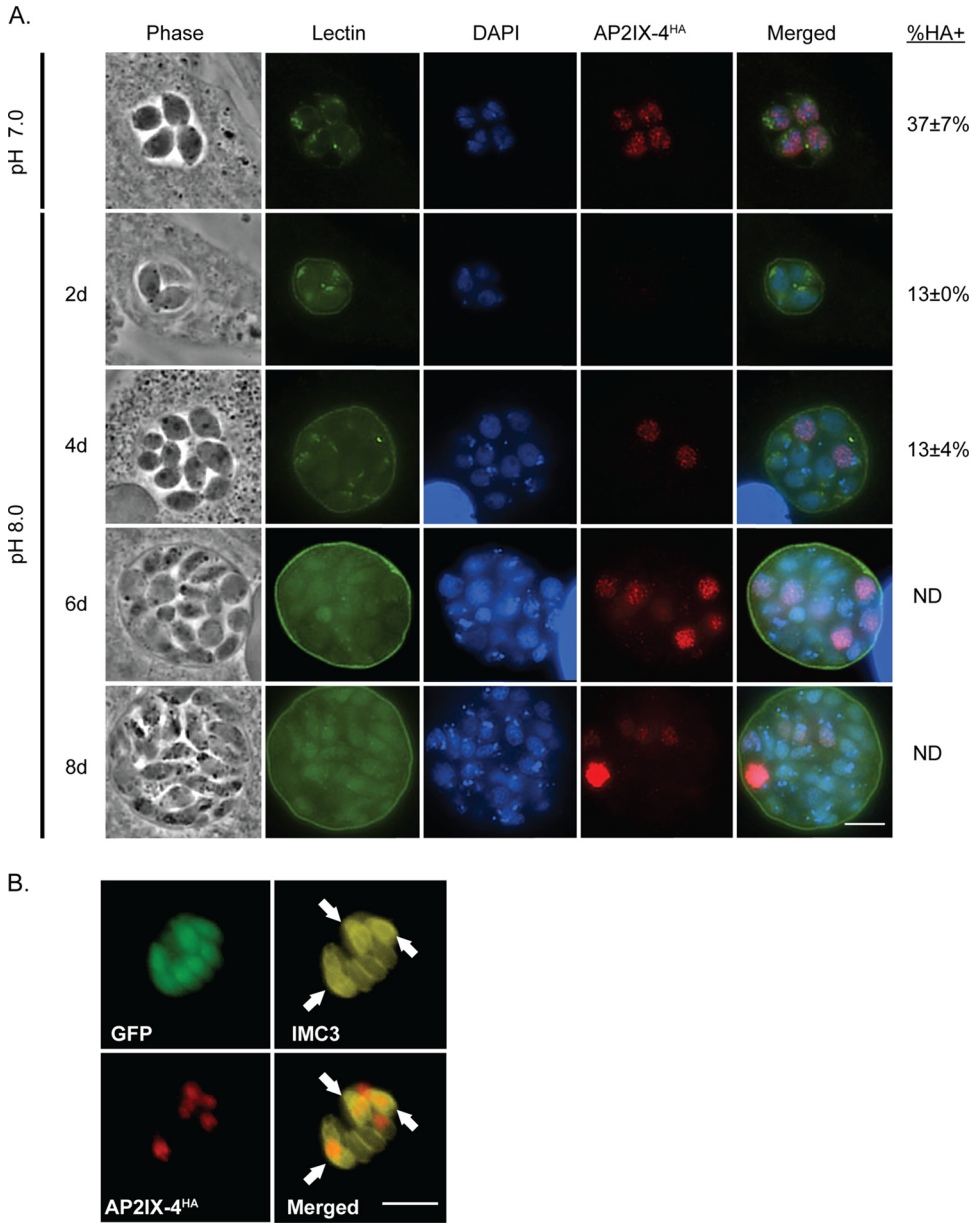

FIG 4 Expression of AP2IX-4 in developing bradyzoites *in vitro*. (A) IFAs were performed on Δ*ap2IX-4*::AP2IX-4^{HA} parasites during the tachyzoite and developing bradyzoite stages for up to 8 days (8d) in alkaline pH. FITC-conjugated *Dolichos* lectin was used to visualize bradyzoite cyst walls (the LDH2-GFP reporter also appears in bradyzoites in this channel). AP2IX-4^{ha} protein was visualized using anti-HA (red), and DAPI (blue) was used to stain DNA. The percentage of parasites expressing AP2IX-4^{HA} within 50 random vacuoles (%HA+) was recorded; note that it was not possible to accurately discern the total number of parasites in tissue cysts beyond 4 days postinduction. ND, not determined. Values represent the averages and standard deviations of results from 3 independent experiments. (B) IFAs performed with anti-IMC3 antibody (yellow) on Δ*ap2IX-4*::AP2IX-4^{HA} parasites following 4 days in alkaline pH. The LDH2-GFP reporter (green) identifies bradyzoites. AP2IX-4^{ha} protein was visualized using anti-HA (red). Arrows point to budding daughter cells in dividing parasites expressing AP2IX-4^{HA}. Scale bar, 3 μm.

4 days in alkaline pH, 73% of parental PruQ parasites converted into bradyzoites, but this was reduced to 46% in parasites lacking AP2IX-4 (Fig. 5). Complementation of the AP2IX-4 knockout parasites restored the rate of bradyzoite cyst formation to levels matching wild-type PruQ strain levels (Fig. 5). These data show that AP2IX-4^{HA} continues to be expressed in a cell cycle-regulated manner post-bradyzoite induction and that its ablation impairs the frequency at which cysts form *in vitro*.

Loss of AP2IX-4 results in dysregulated gene expression. To assess the impact of AP2IX-4 on gene expression, RNA was harvested from parental PruQ and PruQΔ*ap2IX-4*

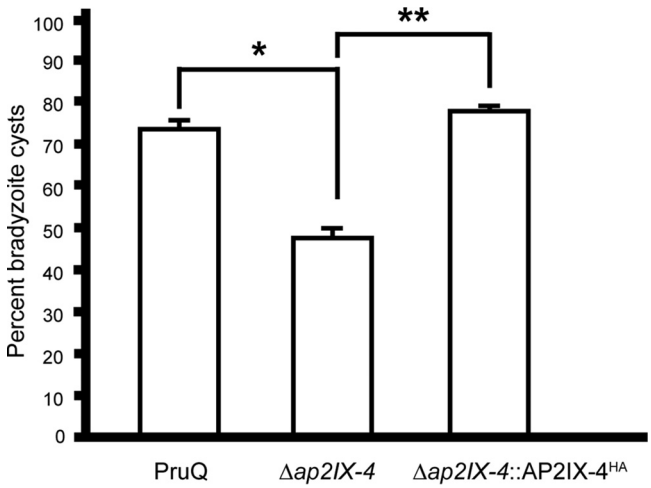

FIG 5 Loss of AP2IX-4 results in lower frequency of bradyzoite cyst formation *in vitro*. Parental PruQ, Δ*ap2IX-4*, and Δ*ap2IX-4*::AP2IX-4^{HA} parasites were cultured in alkaline medium for 4 days and then stained with *Dolichos* lectin to visualize tissue cyst walls. For each sample, 100 random vacuoles were surveyed for the presence or absence of lectin staining to determine the frequency of cyst formation. $n = 4$ for parental and Δ*ap2IX-4*; $n = 3$ for Δ*ap2IX-4*::AP2IX-4^{HA}. *, $P = 0.04$; **, $P = 0.006$ (unpaired two-tailed Student's *t* test). Error bars represent standard errors of the means.

parasites cultured under tachyzoite (pH 7) or bradyzoite-inducing (pH 8.2) conditions for 2 days and hybridized onto ToxoGeneChip microarrays (35). Under tachyzoite conditions, very few genes were dysregulated in the knockout (see Table S2 in the supplemental material). In contrast to the results seen under tachyzoite culture conditions, 119 genes were differentially expressed ≥2-fold in the knockout under bradyzoite induction conditions: 64 were downregulated in the PruQΔ*ap2IX-4* parasites compared to the parental parasites, while 55 were upregulated (Table S3). Approximately 89% of these genes were complemented in knockout parasites in which AP2IX-4 expression had been restored. Table 1 shows a representative group of genes that were rescued by complementation (the complete list of complemented genes is in Table S3).

Four bradyzoite-associated genes, including those encoding enoyl-coenzyme A (enoyl-CoA) hydratase/isomerase and hypothetical proteins TGME49_205680, TGME49_287040, and TGME49_306270, were downregulated in the knockout following stress (Table 1). Enoyl-CoA hydratase/isomerase, along with a MoeA domain-containing protein (involved in biosynthesis of molybdopterin), was downregulated in the AP2IX-4 knockout under both tachyzoite and bradyzoite-inducing conditions. Strikingly, the majority of genes showing enhanced expression in the AP2IX-4 knockout upon stress were those encoding well-established bradyzoite-associated proteins such as ENO1, BAG1, PMA1, B-NTPase, LDH2, DnaK-TPR, SAG2C, and MCP4 (Table 1).

Findings from the transcriptomic analysis suggest that AP2IX-4 leads to aberrant gene expression that is more pronounced following alkaline stress treatment. The overall pattern that emerged suggests that bradyzoite-associated genes generally see enhanced activation in the knockout following stress. To determine if the dysregulated gene expression caused by ablation of AP2IX-4 has consequences on pathogenesis, we examined acute and chronic infection in a mouse model.

Analysis of PruQΔ*ap2IX-4* in mouse models of acute and chronic toxoplasmosis. To determine if the loss of AP2IX-4 impacts virulence *in vivo*, BALB/c mice (8 per group) were infected with 10^7, 10^6, or 10^5 parental PruQ, PruQΔ*ap2IX-4*, or PruQΔ*ap2IX-4*::AP2IX-4^{HA} parasites and monitored for 14 days. A dose of 10^7 parasites was equally lethal for all strains injected into the mice, whereas all mice infected with 10^5 parasites survived (Fig. 6A). Three of the 8 mice infected with either parental or PruQΔ*ap2IX-4*::AP2IX-4^{HA} parasites survived a dosage of 10^6; however, all 8 mice infected with 10^6 of the PruQΔ*ap2IX-4* parasites survived (Fig. 6A). Despite its being dispensable for

TABLE 1 Differentially expressed genes in Δ*ap2IX-4* and Δ*ap2IX-4*::AP2IX-4^{HA} parasites under bradyzoite induction conditions[a]

Accession no.	Annotation	FC	
		PruQΔ*ap2IX-4* mutant versus PruQ parental strain	Δ*ap2IX-4*::AP2IX-4^{HA} mutant versus PruQΔ*ap2IX-4* mutant
Downregulated genes			
TGME49_288950	AP2IX-4	−38.1	22.00
TGME49_319890	Hypothetical protein	−7.6	1.8
TGME49_293480	MoeA N-terminal region (domain I and II) domain-containing protein	−7.4	3.4
TGME49_243940	Hypothetical protein	−7.0	1.8
TGME49_204050	Subtilisin SUB1 (SUB1)	−4.9	1.7
TGME49_317705	Enoyl-CoA hydratase/isomerase	−3.8	2.2
TGME49_297910	Hypothetical protein	−3.7	2.1
TGME49_256792	Hypothetical protein	−3.6	2.1
TGME49_217400	Hypothetical protein	−3.5	3.2
TGME49_205680	Hypothetical protein	−3.2	1.7
TGME49_287040	Hypothetical protein	−3.1	1.8
TGME49_306270	Hypothetical protein	−3.0	1.7
TGME49_280500	Inorganic anion transporter, sulfate permease (SulP) family protein	−2.6	2.2
TGME49_261250	Histone H2A1	−2.6	1.7
TGME49_240090	Rhoptry kinase family protein ROP34, putative	−2.5	1.6
TGME49_214190	SRS46	−2.3	1.6
TGME49_239260	Histone H4	−2.2	1.7
TGME49_261240	Histone H3	−2.1	2.4
TGME49_305160	Histone H2Ba	−2.0	2.9
TGME49_255060	Cytochrome *b* (N-terminal)/b6/petB subfamily protein	−2.0	3.9
Upregulated genes			
TGME49_268860	ENO1	10.2	−2.3
TGME49_312905	Hypothetical protein	9.7	−7.3
TGME49_209755	Hypothetical protein	7.0	−2.5
TGME49_259020	BAG1	5.7	−1.6
TGME49_293790	Hypothetical protein	4.9	−2.1
TGME49_278080	*Toxoplasma gondii* family A protein	4.9	−1.7
TGME49_216140	Tetratricopeptide repeat-containing protein	4.4	−1.8
TGME49_252640	P-type ATPase PMA1	4.4	−1.7
TGME49_225290	GDA1/CD39 (nucleoside phosphatase) (B-NTPase)	4.1	−2.1
TGME49_315560	ATP-binding cassette G family transporter ABCG77	4.0	−1.5
TGME49_291040	Lactate dehydrogenase LDH2 (LDH2)	4.0	−1.6
TGME49_202020	DnaK-tetratricopeptide repeat (DnaK-TPR)	3.9	−1.8
TGME49_221550	CMGC kinase, MAPK family, MEK kinase related	3.7	1.9
TGME49_292260	SAG-related sequence SRS36B (SAG5D)	3.6	−1.9
TGME49_266700	Hypothetical protein	3.5	−1.9
TGME49_240470	Hypothetical protein	3.2	−1.7
TGME49_207160	SAG-related sequence SRS49D (SAG2C)	3.1	−2.2
TGME49_267470	Cold-shock DNA-binding domain-containing protein	3.1	−1.7
TGME49_253680	Hypothetical protein	3.0	1.5
TGME49_208730	Microneme protein, putative (MCP4)	3.0	−1.6
TGME49_207150	SAG-related sequence SRS49C (SAG2D)	2.9	−1.9
TGME49_287960	Hypothetical protein	2.7	−1.6
TGME49_218470	Protein disulfide-isomerase	2.6	1.9
TGME49_253710	Hypothetical protein	2.6	−1.7
TGME49_306338	Dynein gamma chain, flagellar outer arm, putative	2.5	−1.9
TGME49_243720	Peroxisomal biogenesis factor PEX11 (PEX11)	2.5	−1.9
TGME49_259960	Nucleoside diphosphatase	2.4	−1.5
TGME49_312905	Hypothetical protein	2.4	−2.0
TGME49_314250	Bradyzoite rhoptry protein BRP1 (BRP1)	2.4	−1.8
TGME49_253330	Rhoptry kinase family protein (BPK1)	2.3	−1.5
TGME49_224830	Hypothetical protein	2.2	1.5
TGME49_221840	Hypothetical protein	2.2	−1.5
TGME49_311370	Methylmalonate-semialdehyde dehydrogenase	2.1	−2.0
TGME49_213460	Hypothetical protein	2.0	−1.7
TGME49_266900	Cyclin, N-terminal domain-containing protein	2.0	−1.6

[a]Differentially expressed genes were defined as those corresponding to a fold change (FC) difference of ≥2. Genes that were previously found to be upregulated during bradyzoite induction are highlighted in gray (see Materials and Methods).

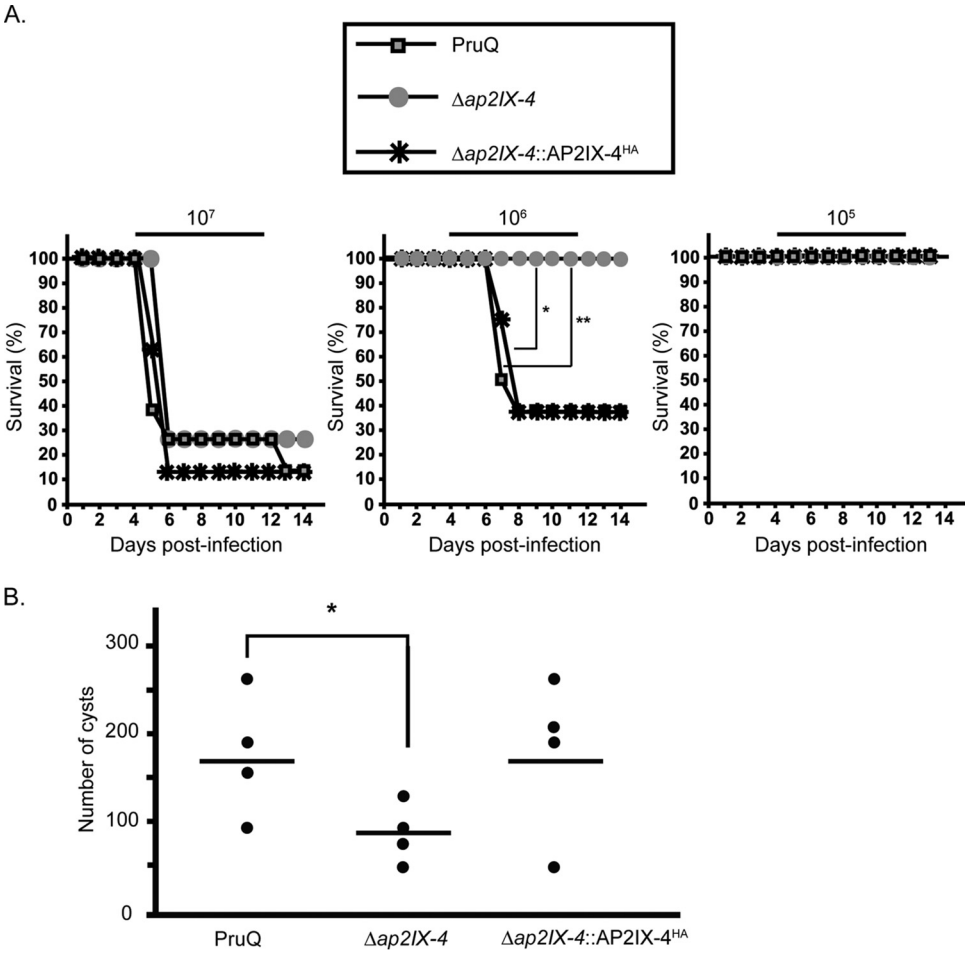

FIG 6 Virulence and cyst burden in mice infected with Δ*ap2IX-4* parasites. (A) Mice ($n = 8$ per group) were infected with 10^7, 10^6, or 10^5 parental, Δ*ap2IX-4*, or Δ*ap2IX-4*::AP2IX-4^{HA} parasites and monitored over 14 days for survival. *, $P = 0.01$; **, $P = 0.02$ (log-rank test). (B) Mice were infected with 10^6 of the designated parasites ($n = 4$ per group) and allowed to progress to chronic infection for 35 days before brain cyst burden was assessed. *, $P = 0.03$ (unpaired one-tailed Student's *t* test).

tachyzoite replication *in vitro*, these data suggest that loss of AP2IX-4 results in a modest virulence defect *in vivo*.

We also analyzed the brain cyst burden in BALB/c mice infected with 10^6 parental PruQ, PruQΔ*ap2IX-4*, or PruQΔ*ap2IX-4*::AP2IX-4HA parasites at 35 days postinfection. Mice infected with parental parasites contained an average of 169 ± 27 brain cysts, while those infected with PruQΔ*ap2IX-4* yielded a significantly reduced average of 91 ± 17 brain cysts ($P = 0.03$; Fig. 6B). Complementation of PruQΔ*ap2IX-4* reversed the phenotype, producing an average of 176 ± 44 brain cysts (Fig. 6B). The restoration of parent levels of cyst formation following complementation indicates successful genetic rescue of PruQΔ*ap2IX-4* defects. This experiment was repeated to ensure reproducibility and yielded a similar trend, with parental parasites producing 4,021 ± 1,488 brain cysts and PruQΔ*ap2IX-4* parasites producing only 487 ± 31 brain cysts ($P = 0.02$; data not shown). Consistent with the reduced frequency of bradyzoite development noted *in vitro*, these data suggest that loss of AP2IX-4 also results in decreased bradyzoite frequency *in vivo*.

DISCUSSION

The establishment of tissue cysts within host cells is essential for *Toxoplasma* transmission and is the underlying cause of chronic infection in patients. Tissue cyst formation requires that tachyzoites slow their replication rate, which is associated with

a lengthening of the G_1 phase (36). A complete inhibition of tachyzoite growth blocks bradyzoite development (37), while no fast-growing bradyzoite has ever been identified. These observations suggest that formation of bradyzoites is a stepwise process involving growth mechanisms, although how many steps and what molecular mechanisms are involved is not understood. At a minimum, tissue cyst development involves a slow-growing prebradyzoite that expresses bradyzoite antigens and a mature stage that is nonreplicative and may be required for transmission (13, 38). Defining the bradyzoite developmental pathway is hampered by its heterologous nature. Unlike the tachyzoite stage, which shows striking synchronous intravacuolar behavior, parasites undergoing bradyzoite development are largely asynchronous and tissue cysts contain a highly variable number of bradyzoites (38). These challenges have contributed to the lack of mechanistic knowledge of how tissue cysts are formed.

Like all ApiAP2 factors characterized, AP2IX-4 is present exclusively in the nucleus. AP2IX-4 also belongs to the set of cyclically regulated ApiAP2 factors of the tachyzoite (Fig. 1C) (21). AP2IX-4 mRNA and protein are dynamically expressed in the tachyzoite, with peak expression occurring during the S phase and mitosis and cytokinesis; as newly formed tachyzoites emerge (G_1 phase), AP2IX-4 expression falls below detectable limits.

To gain insight into the biological role of AP2IX-4, we generated knockout parasites in both type I RH and type II Pru strains. Surprisingly, AP2IX-4 is not essential for tachyzoite replication, indicating that its role is not in regulating the tachyzoite cell cycle *per se*; however, this factor is required for efficient bradyzoite development *in vitro* and *in vivo*. These data indicate that AP2IX-4 could be required for regulating the transition from the tachyzoite to bradyzoite. Previous studies have demonstrated that spontaneous bradyzoite gene expression occurs during the S/M phase of the tachyzoite cell cycle (21), and the prebradyzoite (SAG1-positive [$SAG1^+$]/$BAG1^+$) transitional stages also show higher numbers of parasites with the characteristic genome content of late S-phase/mitotic parasites (36). AP2IX-4 expression was detected in response to alkaline stress in only a subpopulation of parasites (Fig. 4) that, based on costaining with the daughter budding marker IMC3, were undergoing division. These AP2IX-4 vacuoles were also positive for *Dolichos biflorus* lectin staining, indicating that differentiation of the tissue cyst was also under way (Fig. 4). These findings support the long-held view that bradyzoite development is asynchronous compared to tachyzoite replication (38, 39). The stochastic nature of bradyzoite development is not understood in mechanistic terms; however, ApiAP2 factors such as AP2IX-4 now provide new experimental avenues to help define the individual steps of tissue cyst differentiation at the level of the individual parasite.

Transcriptome analysis of PruQΔ*ap2IX-4* parasites shed further light on AP2IX-4 function. Consistent with a presumed lack of a role in tachyzoite cell division, no significant differences were determined between the Pru parent and AP2IX-4 knockout tachyzoites (grown in normal pH 7.0 media). However, in response to alkaline stress, numerous bradyzoite-specific mRNAs exhibited greatly enhanced expression when AP2IX-4 was disrupted (Table 1), with the vast majority (~90%) of these gene expression changes reversed following complementation. As only ~13% of encysted parasites were expressing AP2IX-4 (Fig. 4), it is likely that the lack of synchronization in the microarray study underestimated the magnitude and number of genes regulated by this factor. Nevertheless, our transcriptomic analysis indicates that AP2IX-4 primarily functions to repress a subset of bradyzoite genes during the early stages of bradyzoite development. In addition to metabolic genes known to be specifically expressed in the bradyzoite, AP2IX-4 may also control a novel, bradyzoite-specific CMGC (cyclin-dependent kinase [CDK], mitogen-activated protein kinase [MAPK], glycogen synthase kinase [GSK3], CDC-like kinase [CLK]) kinase that may play a role in stress-induced signal transduction promoting latency. Altogether, these data reveal that what is distinctive about AP2IX-4 is its role in balancing the induction of gene expression in stress-induced bradyzoites, while having no apparent function in regulating gene expression specific to the tachyzoite.

This pattern of gene expression in AP2IX-4 knockout parasites is not the classic profile of a transcriptional repressor, where misexpression of bradyzoite genes in the tachyzoite would be expected. In a separate study, we have identified a bradyzoite transcriptional repressor in the tachyzoite that fits this classic pattern (40).

Like AP2IX-4, AP2IV-4 exhibits peak expression in the tachyzoite S/M phase; however, dysregulated expression of bradyzoite-associated mRNAs in an AP2IV-4 knockout occurs without stress. In contrast, AP2IX-4 may act as a passive repressor (i.e., it may suppress transcription by competing with an activator for its target binding site) that requires an additional protein induced by alkaline stress (41). Both types of repressors (active and passive) are well documented among the AP2 transcription factors of plants (41). Alternatively, AP2IX-4 could be a weak transcriptional activator that works in conjunction with a stronger activator to express bradyzoite mRNAs at the proper level and time. In the absence of AP2IX-4 to regulate a stronger transcription factor, the timing of expression for a subset of bradyzoite-associated genes could become unbalanced, leading to the negative effects on tissue cyst development that we have observed *in vitro* and *in vivo*. In addition, the unbalancing of gene expression during bradyzoite development caused by the loss of AP2IX-4 could cause problems either with tissue-specific formation of the tissue cyst or in achieving the proper escape from the host immune system. Preventing the prearming of the immune system against the parasite surviving to form the tissue cyst is a confirmed function for AP2IV-4 (40) and likely has driven the evolution of AP2IX-4 function. Validating this function will require a complete dissection of the AP2IX-4 transcriptional mechanism and its molecular partners during bradyzoite development *in vitro* and *in vivo*.

Our recent studies, and other investigations, have uncovered a number of ApiAP2s that modulate gene expression associated with the developmental transition between tachyzoites and bradyzoites. The AP2IX-4 studied here joins this list of factors. AP2IX-9 represses the expression of bradyzoite mRNAs; overexpression of AP2IX-9 promotes tachyzoite growth during stress and prevents formation of tissue cysts (23). AP2IV-4 is a cell cycle-regulated factor with peak expression in the tachyzoite S/M phase that also suppresses bradyzoite gene expression (40). In contrast, AP2IV-3 is an activator of bradyzoite gene expression; a knockout reduces tissue cyst formation, and its overexpression increases tissue cyst formation (26). Changes in bradyzoite gene expression also occurred following the deletion of AP2XI-4, suggesting that this factor could be a transcriptional activator of bradyzoite gene expression (24). Thus, the model emerging from recent studies suggests that ApiAP2s act within a complex transcriptional network comprised of activators and repressors that operate at the interface of tachyzoite replication and bradyzoite conversion in order to control the intermediate life cycle. The presence of multiple levels of ApiAP2 factor regulation in bradyzoite development contrasts with the "master regulatory factor" model of gametogenesis of *Plasmodium falciparum* (20). *Toxoplasma* has more than twice as many ApiAP2 factors as *P. falciparum* and a much larger number of hosts that can serve the *Toxoplasma* intermediate life cycle. Consistent with this life cycle flexibility, a recent analysis of ApiAP2 factor expression revealed that a larger number of ApiAP2 factors are expressed in the intermediate life cycle (26). Therefore, it is reasonable to suggest that the large diversity of *Toxoplasma* ApiAP2 factors regulating bradyzoite development was necessary to expand the host range of the intermediate life cycle. Future studies focused on how *Toxoplasma* ApiAP2 factors function in different animal hosts will be important to understand how these transcriptional mechanisms evolved.

MATERIALS AND METHODS

Parasite culture and growth assays. Parasite strains used in these studies included the RHΔ*ku80*::HXGPRT (RHQ) and PruΔ*ku80*Δ*hxgprt* (PruQ) mutant strains (33, 42, 43). All parasites were cultured in confluent monolayers of human foreskin fibroblasts (HFFs) using Dulbecco's modified Eagle's medium (DMEM) supplemented with 1% and 5% heat-inactivated fetal bovine serum (FBS), respectively. Cultures were maintained in humidified incubators at 37°C with 5% CO_2. Parasite doubling assays were performed as previously described (44). Briefly, 10^6 freshly lysed tachyzoites were inoculated onto host cell monolayers; after 24 h, the number of tachyzoites present within 50 random vacuoles was recorded at

12-h intervals. For plaque assays, infected monolayers in 12-well plates were stained with crystal violet to visualize and count plaques (45).

To initiate conversion to bradyzoites *in vitro*, type II parasites were allowed to invade HFF monolayers for 4 h under normal culture conditions, and then the medium was replaced with alkaline RPMI medium (pH 8.2) and the cultures were moved to a 37°C incubator with ambient CO_2.

Generation of parasites expressing endogenously tagged AP2IX-4. RHQ parasites were engineered to express endogenous AP2IX-4 tagged at its C terminus with three tandem copies of the hemagglutinin (3xHA) epitope. Modification of the endogenous genomic locus was achieved through allelic replacement using parasites lacking KU80 to facilitate homologous recombination (42, 43). This genetic "knock-in" approach employed the pLIC-3xHA plasmid, which contains a 1,514-bp sequence from the AP2IX-4 locus for homologous recombination (Fig. 1), amplified with primers shown in Table S1 in the supplemental material. This endogenous tagging construct also contains a modified dihydrofolate reductase-thymidylate synthase (DHFR*-TS) minigene that confers resistance to pyrimethamine for selection of transgenic parasites (46). Following drug selection, parasites were cloned by limiting dilution in 96-well plates.

Generation of AP2IX-4 knockout parasites. Deletion of the AP2IX-4 gene was carried out in both RHQ and PruQ parasites. To generate the Δ*ap2IX-4* clones, a plasmid was constructed that flanked the DHFR*-TS minigene with 1.6-kb to 1.9-kb sequences homologous to regions of the AP2IX-4 locus up- and downstream of the coding region (Fig. 2A). This "knockout" plasmid was made using a MultiSite Gateway three-fragment vector construction kit (Invitrogen) based on methods previously described (47). Two entry vectors were constructed to include 5′ and 3′ flanking sequences for recombination with the endogenous locus: pDONR_P2R-P3 contained the 1,875-bp sequence downstream of the AP2IX-4 genomic sequence, and pDONR_P4P1R contained the 1,660-bp sequence upstream. A third entry vector, pDONR221, was constructed to contain the DHFR*-TS minigene. Each entry vector was constructed using the Gateway BP reaction, which consists of combining a PCR product with a pDONR vector; all primers used to generate these vectors are listed in Table S1. The three entry vectors were combined in a Gateway LR reaction with destination vector pDEST_R4R3 to create the final knockout plasmids, which were then electroporated into RHQ or PruQ parasites (45). Pyrimethamine-resistant parasites were cloned by limiting dilution and examined by genomic PCR and RT-PCR to confirm the fidelity of each knockout (Fig. 2B).

Complementation of the AP2IX-4 knockout. We complemented the PruQΔ*ap2IX-4* parasites by restoring a cDNA-derived version of AP2IX-4 at the knockout locus and downstream of its endogenous promoter using single homologous recombination (Fig. 3A). A 2,116-bp sequence upstream of the start codon was amplified (the primers are shown in Table S1) and ligated to a cDNA-derived AP2IX-4 coding sequence using InFusion cloning (Clontech) and integrated at the PacI restriction site into vector pLIC-3HA-HXGPRT. Vector pLIC-3HA-HXGPRT contains the HXGPRT drug selection cassette that replaced the DHFR*-TS minigene of its parental vector, pLIC-3HA-DHFR. Integration of the AP2IX-4 coding sequence into pLIC-3HA-HXGPRT fuses it to a C-terminal 3xHA tag. The resulting plasmid was electroporated into Δ*ap2IX-4* parasites, which were then selected in 25 μg/ml mycophenolic acid and 50 μg/ml xanthine and cloned by limiting dilution (48).

RT-PCR. Total RNA was isolated from the designated parasites using TRIzol reagent (Ambion) and treatment with DNase I (Promega) for 30 min at 37°C. The mRNA was reverse transcribed using Omniscript reverse transcriptase (Qiagen) and oligo(dT) primers per the manufacturer's instructions; subsequent PCRs were performed using primers for AP2IX-4 or GAPDH (glyceraldehyde-3-phosphate dehydrogenase) (Table S1).

Western blot analysis. Immunoblotting of parasite lysate was used to detect AP2IX-4 in various clones by virtue of the 3xHA epitope tag. Parasite lysate was prepared in lysis buffer (150 mM NaCl, 50 mM Tris-Cl [pH 7.5], 0.1% NP-40) and sonicated prior to resolution on SDS-PAGE and transfer to a nitrocellulose membrane. HA epitopes were detected using rat anti-HA antibody (Roche) at a 1:5,000 dilution followed by secondary probing with horseradish peroxidase (HRP)-conjugated goat anti-rat antibody (GE Healthcare) at a 1:2,000 dilution. To ensure equal loading of samples, we also probed with rabbit anti-β-tubulin antibody (kindly supplied by David Sibley, Washington University) at a 1:2,000 dilution followed by HRP-conjugated donkey anti-rabbit antibody (GE Healthcare) at a 1:2,000 dilution.

Immunofluorescence assays (IFA). HFF monolayers grown on coverslips in 12-well plates were inoculated with freshly lysed parasites. Infected monolayers were fixed in 3% paraformaldehyde (PFA) for 10 min, quenched in 0.1 M glycine for 5 min, and then permeabilized with 0.3% Triton X-100 for 20 min with blocking in 3% bovine serum albumin (BSA)–1× phosphate-buffered saline (PBS) for 30 min. For IFAs of tachyzoite cultures, rabbit polyclonal anti-HA primary antibody (Invitrogen) was applied at a 1:2,000 dilution overnight at 4°C, followed by goat anti-rabbit Alexa Fluor 488 secondary antibody (Thermo Fisher) at a 1:4,000 dilution. Detection of IMC3 was achieved using rat monoclonal anti-IMC3 antibody (kindly supplied by Marc-Jan Gubbels, Boston College) at a 1:2,000 dilution overnight at 4°C, followed by goat anti-rat Alexa Fluor 594 antibody (Thermo Fisher) at a 1:4,000 dilution. 4′,6-Diamidino-2-phenylindole (DAPI; Vector Laboratories) was applied for 5 min as a costain to visualize nuclei. For IFAs of bradyzoite cultures, rat monoclonal anti-HA primary antibody (Roche) was applied at a 1:1,000 dilution for 1 h at room temperature, followed by goat anti-rat Alexa Fluor 594 secondary antibody at a 1:1,000 dilution. For the visualization of tissue cyst walls, fluorescein isothiocyanate (FITC)- or rhodamine-conjugated *Dolichos biflorus* lectin (Vector Laboratories) was applied at a 1:1,000 dilution for 30 min at room temperature or at a 1:250 dilution overnight at 4°C, respectively. In IFAs costained for IMC3 or SAG1, rabbit polyclonal anti-HA primary antibody was applied at a 1:2,000 dilution, followed by goat anti-rabbit Alexa Fluor 568 secondary antibody at a 1:4,000 dilution. Detection of IMC3 was achieved

using rat monoclonal anti-IMC3 antibody at a 1:2,000 dilution overnight at 4°C, followed by either goat anti-rat Alexa Fluor 647 antibody or goat anti-rat Alexa Fluor 594 antibody at a 1:4,000 dilution. Detection of SAG1 was achieved using mouse monoclonal anti-SAG1 antibody (Abcam, Inc.) followed by goat anti-mouse Alexa Fluor 647 secondary antibody.

RNA purification and microarray analyses. Tachyzoite total RNA was purified from intracellular PruQ or Δ*ap2IX-4* parasites maintained at pH 7.0 (32 to 36 h postinfection) or PruQ, PruQΔ*ap2IX-4*, or PruQΔ*ap2IX-4*::AP2IX-4^{HA} parasites maintained at pH 8.2 (48 h) using an RNeasy minikit (Qiagen) according to the manufacturer's instructions. Intracellular tachyzoites or induced bradyzoites were harvested by scraping the monolayer and passage of the culture through a syringe with a 27-gauge needle. Host cell debris was excluded using a 3-μm-pore-size filter for tachyzoites and a 5-μm-pore-size filter for bradyzoites. Two biological replicates were prepared for each parasite line under each set of experimental conditions, and RNA quality was assessed using an Agilent Bioanalyzer 2100 (Santa Cruz, CA). RNA samples were prepared for hybridization on a ToxoGeneChip as previously described (21). Hybridization data were analyzed using the GeneSpring GX software package (v12.6.1; Agilent), and all data sets have been made available in the NCBI GEO database. Transcriptome data from previous publications were used to determine whether the genes in our data sets were associated with expression in the bradyzoite stage (31, 49).

Virulence and cyst burden in infected mice. To examine acute virulence, 5-to-6-week-old female BALB/c mice were injected intraperitoneally with 10^5, 10^6, or 10^7 parental PruQ, PruQΔ*ap2IX-4*, or PruQΔ*ap2IX-4*::AP2IX-4^{HA} parasites (8 mice per group). Plaque assays were performed for each sample and ensured equal levels of viability between strains. Mice were examined daily, and time to death was recorded. Serology performed on cardiac bleeds of infected mice confirmed the presence of *Toxoplasma*. To assess the cyst burden, mice were infected with 10^6 parasites as described above and allowed to progress to chronic infection for 35 days (4 mice per group). Brains were then homogenized; homogenates were fixed, quenched, and permeabilized. Samples were blocked in 3% BSA–1× PBS–0.2% Triton X-100. To visualize cyst walls, rhodamine-conjugated *Dolichos biflorus* lectin (Vector Laboratories) was applied at a 1:250 dilution overnight at 4°C. Cyst quantification was performed as previously described (50).

Ethics statement. Mice were infected with *Toxoplasma* using an approved protocol (10852) from the Institutional Animal Care and Use Committee (IACUC) of the Indiana University School of Medicine (IUSM). The IUSM is accredited by the International Association for Assessment and Accreditation of Laboratory Animal Care.

Accession number(s). All data sets from this work have been made available in the NCBI GEO database (GSE94045).

SUPPLEMENTAL MATERIAL

Supplemental material for this article may be found at https://doi.org/10.1128/mSphere.00054-17.

TABLE S1, XLSX file, 0.01 MB.

TABLE S2, XLSX file, 0.01 MB.

TABLE S3, XLSX file, 0.02 MB.

ACKNOWLEDGMENTS

We thank David Sibley (Washington University) and Marc-Jan Gubbels (Boston College) for donating antibody reagents, Gustavo Arrizabalaga (Indiana University School of Medicine) for helpful discussions, and Gian Gballou for assisting with cyst burden quantification. We also thank Joanna Gress at the Functional Genomics Core Facility at Montana State University for help with hybridization of the ToxoGeneChip microarrays.

This research was supported by Showalter Scholar Funding (to W.J.S., Jr.) and the National Institutes of Health (AI089885 and AI124682 to M.W.W.). The funders had no role in study design, data collection and interpretation, or the decision to submit the work for publication.

REFERENCES

1. Hill DE, Chirukandoth S, Dubey JP. 2005. Biology and epidemiology of Toxoplasma gondii in man and animals. Anim Health Res Rev 6:41–61. https://doi.org/10.1079/AHR2005100.
2. Sullivan WJ, Jr, Jeffers V. 2012. Mechanisms of Toxoplasma gondii persistence and latency. FEMS Microbiol Rev 36:717–733. https://doi.org/10.1111/j.1574-6976.2011.00305.x.
3. Dubey JP. 1998. Toxoplasma gondii oocyst survival under defined temperatures. J Parasitol 84:862–865. https://doi.org/10.2307/3284606.
4. Dubey JP, Jones JL. 2008. Toxoplasma gondii infection in humans and animals in the United States. Int J Parasitol 38:1257–1278. https://doi.org/10.1016/j.ijpara.2008.03.007.
5. Hill D, Dubey JP. 2002. Toxoplasma gondii: transmission, diagnosis and prevention. Clin Microbiol Infect 8:634–640. https://doi.org/10.1046/j.1469-0691.2002.00485.x.
6. Montoya JG, Liesenfeld O. 2004. Toxoplasmosis. Lancet 363:1965–1976. https://doi.org/10.1016/S0140-6736(04)16412-X.
7. Behnke MS, Radke JB, Smith AT, Sullivan WJ, Jr, White MW. 2008. The transcription of bradyzoite genes in Toxoplasma gondii is controlled by

autonomous promoter elements. Mol Microbiol 68:1502–1518. https://doi.org/10.1111/j.1365-2958.2008.06249.x.
8. Balaji S, Babu MM, Iyer LM, Aravind L. 2005. Discovery of the principal specific transcription factors of Apicomplexa and their implication for the evolution of the AP2-integrase DNA binding domains. Nucleic Acids Res 33:3994–4006. https://doi.org/10.1093/nar/gki709.
9. Riechmann JL, Meyerowitz EM. 1998. The AP2/EREBP family of plant transcription factors. Biol Chem 379:633–646.
10. Woo YH, Ansari H, Otto TD, Klinger CM, Kolisko M, Michálek J, Saxena A, Shanmugam D, Tayyrov A, Veluchamy A, Ali S, Bernal A, del Campo J, Cihlář J, Flegontov P, Gornik SG, Hajdušková E, Horák A, Janouškovec J, Katris NJ, Mast FD, Miranda-Saavedra D, Mourier T, Naeem R, Nair M, Panigrahi AK, Rawlings ND, Padron-Regalado E, Ramaprasad A, Samad N, Tomčala A, Wilkes J, Neafsey DE, Doerig C, Bowler C, Keeling PJ, Roos DS, Dacks JB, Templeton TJ, Waller RF, Lukes J, Obornik M, Pain A. 2015. Chromerid genomes reveal the evolutionary path from photosynthetic algae to obligate intracellular parasites. Elife 4:e06974. https://doi.org/10.7554/eLife.06974.
11. Oberstaller J, Pumpalova Y, Schieler A, Llinás M, Kissinger JC. 2014. The Cryptosporidium parvum ApiAP2 gene family: insights into the evolution of apicomplexan AP2 regulatory systems. Nucleic Acids Res 42:8271–8284. https://doi.org/10.1093/nar/gku500.
12. Painter HJ, Campbell TL, Llinás M. 2011. The apicomplexan AP2 family: integral factors regulating plasmodium development. Mol Biochem Parasitol 176:1–7. https://doi.org/10.1016/j.molbiopara.2010.11.014.
13. White MW, Radke JR, Radke JB. 2014. Toxoplasma development—turn the switch on or off? Cell Microbiol 16:466–472. https://doi.org/10.1111/cmi.12267.
14. Pieszko M, Weir W, Goodhead I, Kinnaird J, Shiels B. 2015. ApiAP2 factors as candidate regulators of stochastic commitment to merozoite production in Theileria annulata. PLoS Negl Trop Dis 9:e0003933. https://doi.org/10.1371/journal.pntd.0003933.
15. Yuda M, Iwanaga S, Shigenobu S, Mair GR, Janse CJ, Waters AP, Kato T, Kaneko I. 2009. Identification of a transcription factor in the mosquito-invasive stage of malaria parasites. Mol Microbiol 71:1402–1414. https://doi.org/10.1111/j.1365-2958.2009.06609.x.
16. Yuda M, Iwanaga S, Shigenobu S, Kato T, Kaneko I. 2010. Transcription factor AP2-Sp and its target genes in malarial sporozoites. Mol Microbiol 75:854–863. https://doi.org/10.1111/j.1365-2958.2009.07005.x.
17. Iwanaga S, Kaneko I, Kato T, Yuda M. 2012. Identification of an AP2-family protein that is critical for malaria liver stage development. PLoS One 7:e47557. https://doi.org/10.1371/journal.pone.0047557.
18. Sinha A, Hughes KR, Modrzynska KK, Otto TD, Pfander C, Dickens NJ, Religa AA, Bushell E, Graham AL, Cameron R, Kafsack BF, Williams AE, Llinás M, Berriman M, Billker O, Waters AP. 2014. A cascade of DNA-binding proteins for sexual commitment and development in plasmodium. Nature 507:253–257. https://doi.org/10.1038/nature12970.
19. Yuda M, Iwanaga S, Kaneko I, Kato T. 2015. Global transcriptional repression: an initial and essential step for plasmodium sexual development. Proc Natl Acad Sci U S A 112:12824–12829. https://doi.org/10.1073/pnas.1504389112.
20. Kafsack BF, Rovira-Graells N, Clark TG, Bancells C, Crowley VM, Campino SG, Williams AE, Drought LG, Kwiatkowski DP, Baker DA, Cortés A, Llinás M. 2014. A transcriptional switch underlies commitment to sexual development in malaria parasites. Nature 507:248–252. https://doi.org/10.1038/nature12920.
21. Behnke MS, Wootton JC, Lehmann MM, Radke JB, Lucas O, Nawas J, Sibley LD, White MW. 2010. Coordinated progression through two subtranscriptomes underlies the tachyzoite cycle of Toxoplasma gondii. PLoS One 5:e12354. https://doi.org/10.1371/journal.pone.0012354.
22. Wang J, Dixon SE, Ting LM, Liu TK, Jeffers V, Croken MM, Calloway M, Cannella D, Hakimi MA, Kim K, Sullivan WJ, Jr. 2014. Lysine acetyltransferase GCN5b interacts with AP2 factors and is required for Toxoplasma gondii proliferation. PLoS Pathog 10:e1003830. https://doi.org/10.1371/journal.ppat.1003830.
23. Radke JB, Lucas O, De Silva EK, Ma Y, Sullivan WJ, Jr, Weiss LM, Llinas M, White MW. 2013. ApiAP2 transcription factor restricts development of the toxoplasma tissue cyst. Proc Natl Acad Sci U S A 110:6871–6876. https://doi.org/10.1073/pnas.1300059110.
24. Walker R, Gissot M, Croken MM, Huot L, Hot D, Kim K, Tomavo S. 2013. The toxoplasma nuclear factor TgAP2XI-4 controls bradyzoite gene expression and cyst formation. Mol Microbiol 87:641–655. https://doi.org/10.1111/mmi.12121.
25. Lescault PJ, Thompson AB, Patil V, Lirussi D, Burton A, Margarit J, Bond J, Matrajt M. 2010. Genomic data reveal Toxoplasma gondii differentiation mutants are also impaired with respect to switching into a novel extracellular tachyzoite state. PLoS One 5:e14463. https://doi.org/10.1371/journal.pone.0014463.
26. Hong D-P, Radke JB, White MW. 2016. Opposing transcriptional mechanisms regulate toxoplasma development. bioRxiv https://doi.org/10.1101/094847.
27. Letunic I, Doerks T, Bork P. 2012. SMART 7: recent updates to the protein domain annotation resource. Nucleic Acids Res 40:D302–D305. https://doi.org/10.1093/nar/gkr931.
28. Mitchell A, Chang HY, Daugherty L, Fraser M, Hunter S, Lopez R, McAnulla C, McMenamin C, Nuka G, Pesseat S, Sangrador-Vegas A, Scheremetjew M, Rato C, Yong SY, Bateman A, Punta M, Attwood TK, Sigrist CJ, Redaschi N, Rivoire C, Xenarios I, Kahn D, Guyot D, Bork P, Letunic I, Gough J, Oates M, Haft D, Huang H, Natale DA, Wu CH, Orengo C, Sillitoe I, Mi H, Thomas PD, Finn RD. 2015. The InterPro protein families database: the classification resource after 15 years. Nucleic Acids Res 43:D213–D221. https://doi.org/10.1093/nar/gku1243.
29. Gubbels MJ, Wieffer M, Striepen B. 2004. Fluorescent protein tagging in Toxoplasma gondii: identification of a novel inner membrane complex component conserved among Apicomplexa. Mol Biochem Parasitol 137:99–110. https://doi.org/10.1016/j.molbiopara.2004.05.007.
30. Radke JR, Striepen B, Guerini MN, Jerome ME, Roos DS, White MW. 2001. Defining the cell cycle for the tachyzoite stage of Toxoplasma gondii. Mol Biochem Parasitol 115:165–175. https://doi.org/10.1016/S0166-6851(01)00284-5.
31. Pittman KJ, Aliota MT, Knoll LJ. 2014. Dual transcriptional profiling of mice and Toxoplasma gondii during acute and chronic infection. BMC Genomics 15:806. https://doi.org/10.1186/1471-2164-15-806.
32. Soête M, Camus D, Dubremetz JF. 1994. Experimental induction of bradyzoite-specific antigen expression and cyst formation by the RH strain of Toxoplasma gondii in vitro. Exp Parasitol 78:361–370. https://doi.org/10.1006/expr.1994.1039.
33. Fox BA, Falla A, Rommereim LM, Tomita T, Gigley JP, Mercier C, Cesbron-Delauw MF, Weiss LM, Bzik DJ. 2011. Type II Toxoplasma gondii KU80 knockout strains enable functional analysis of genes required for cyst development and latent infection. Eukaryot Cell 10:1193–1206. https://doi.org/10.1128/EC.00297-10.
34. Singh U, Brewer JL, Boothroyd JC. 2002. Genetic analysis of tachyzoite to bradyzoite differentiation mutants in Toxoplasma gondii reveals a hierarchy of gene induction. Mol Microbiol 44:721–733. https://doi.org/10.1046/j.1365-2958.2002.02903.x.
35. Bahl A, Davis PH, Behnke M, Dzierszinski F, Jagalur M, Chen F, Shanmugam D, White MW, Kulp D, Roos DS. 2010. A novel multifunctional oligonucleotide microarray for Toxoplasma gondii. BMC Genomics 11:603. https://doi.org/10.1186/1471-2164-11-603.
36. Radke JR, Guerini MN, Jerome M, White MW. 2003. A change in the premitotic period of the cell cycle is associated with bradyzoite differentiation in Toxoplasma gondii. Mol Biochem Parasitol 131:119–127. https://doi.org/10.1016/S0166-6851(03)00198-1.
37. Bohne W, Heesemann J, Gross U. 1994. Reduced replication of Toxoplasma gondii is necessary for induction of bradyzoite-specific antigens: a possible role for nitric oxide in triggering stage conversion. Infect Immun 62:1761–1767.
38. Watts E, Zhao Y, Dhara A, Eller B, Patwardhan A, Sinai AP. 2015. Novel approaches reveal that Toxoplasma gondii bradyzoites within tissue cysts are dynamic and replicating entities in vivo. mBio 6:e01155-15. https://doi.org/10.1128/mBio.01155-15.
39. Dzierszinski F, Nishi M, Ouko L, Roos DS. 2004. Dynamics of Toxoplasma gondii differentiation. Eukaryot Cell 3:992–1003. https://doi.org/10.1128/EC.3.4.992-1003.2004.
40. Radke JB, Worth D, Hong D-P, Huang S, Sullivan W, Jr, Wilson EH, White MW. 2017. Transcriptional repression by ApiAP2 factors is central to chronic toxoplasmosis. bioRxiv https://doi.org/10.1101/100628.
41. Licausi F, Ohme-Takagi M, Perata P. 2013. APETALA2/Ethylene Responsive Factor (AP2/ERF) transcription factors: mediators of stress responses and developmental programs. New Phytol 199:639–649. https://doi.org/10.1111/nph.12291.
42. Fox BA, Ristuccia JG, Gigley JP, Bzik DJ. 2009. Efficient gene replacements in Toxoplasma gondii strains deficient for nonhomologous end joining. Eukaryot Cell 8:520–529. https://doi.org/10.1128/EC.00357-08.
43. Huynh MH, Carruthers VB. 2009. Tagging of endogenous genes in a Toxoplasma gondii strain lacking Ku80. Eukaryot Cell 8:530–539. https://doi.org/10.1128/EC.00358-08.

44. Fichera ME, Bhopale MK, Roos DS. 1995. In vitro assays elucidate peculiar kinetics of clindamycin action against Toxoplasma gondii. Antimicrob Agents Chemother 39:1530–1537. https://doi.org/10.1128/AAC.39.7.1530.
45. Roos DS, Donald RG, Morrissette NS, Moulton AL. 1994. Molecular tools for genetic dissection of the protozoan parasite Toxoplasma gondii. Methods Cell Biol 45:27–63.
46. Donald RG, Roos DS. 1993. Stable molecular transformation of Toxoplasma gondii: a selectable dihydrofolate reductase-thymidylate synthase marker based on drug-resistance mutations in malaria. Proc Natl Acad Sci U S A 90:11703–11707. https://doi.org/10.1073/pnas.90.24.11703.
47. Upadhya R, Kim K, Hogue-Angeletti R, Weiss LM. 2011. Improved techniques for endogenous epitope tagging and gene deletion in Toxoplasma gondii. J Microbiol Methods 85:103–113. https://doi.org/10.1016/j.mimet.2011.02.001.
48. Donald RG, Carter D, Ullman B, Roos DS. 1996. Insertional tagging, cloning, and expression of the Toxoplasma gondii hypoxanthine-xanthine-guanine phosphoribosyltransferase gene. Use as a selectable marker for stable transformation. J Biol Chem 271:14010–14019. https://doi.org/10.1074/jbc.271.24.14010.
49. Buchholz KR, Fritz HM, Chen X, Durbin-Johnson B, Rocke DM, Ferguson DJ, Conrad PA, Boothroyd JC. 2011. Identification of tissue cyst wall components by transcriptome analysis of in vivo and in vitro Toxoplasma gondii bradyzoites. Eukaryot Cell 10:1637–1647. https://doi.org/10.1128/EC.05182-11.
50. Lavine MD, Knoll LJ, Rooney PJ, Arrizabalaga G. 2007. A Toxoplasma gondii mutant defective in responding to calcium fluxes shows reduced in vivo pathogenicity. Mol Biochem Parasitol 155:113–122. https://doi.org/10.1016/j.molbiopara.2007.06.004.